Parameter Identification of Pedestrian's Spring-Mass-Damper Model by Ground Reaction Force Records through a Particle Filter Approach

Haoqi Wang[1,2], Jun Chen[1,*], James M. W. Brownjohn[3]

[1]*College of Civil Engineering, Tongji University, Shanghai 200092, China*

[2]*Department of Civil Engineering, The University of Tokyo, Tokyo 113-8656, Japan*

[3]*Vibration Engineering Section, University of Exeter, Exeter EX4 4QF, United Kingdom*

Abstract

The spring-mass-damper (SMD) model with a pair of internal biomechanical forces is the simplest model for a walking pedestrian to represent his/her mechanical properties, and thus can be used in human-structure-interaction analysis in the vertical direction. However, the values of SMD stiffness and damping, though very important, are typically taken as those measured from stationary people due to lack of a parameter identification methods for a walking pedestrian. This study adopts a step-by-step system identification approach known as particle filter to simultaneously identify the stiffness, damping coefficient, and coefficients of the SMD model's biomechanical forces by ground reaction force (GRF) records.

After a brief introduction of the SMD model, the proposed identification approach is explained in detail, with a focus on the theory of particle filter and its integration with the SMD model. A numerical example is first provided to verify the feasibility of the proposed approach which is

* Corresponding Author, cejchen@tongji.edu.cn

then applied to several experimental GRF records. Identification results demonstrate that natural frequency and the damping ratio of a walking pedestrian are not constant but have a dependence of mean value and distribution on pacing frequency. The mean value first-order coefficient of the biomechanical force, which is expressed by the Fourier series function, also has a linear relationship with pacing frequency. Higher order coefficients do not show a clear relationship with pacing frequency but follow a logarithmic normal distribution.

Keywords: Human-induced load, spring-mass-damper model, biomechanical load factor, parameter identification, particle filter

1. Introduction

Long-span civil engineering structures, such as cantilever stands, pedestrian bridges and floors, may experience vibrations when subjected to human-induced dynamic loads due to walking, jumping, etc. When the load's dominant frequency is equal or close to the natural frequency of the structure, resonant or near-resonant vibrations will occur and can be perceptible to occupants. These vibrations can cause occupants to be distracted, dizzy or even terrified if excessive, leading to vibration serviceability problems [1,2], which need to be addressed at the design stage of a vibration-prone structure. An accurate and reliable load model is a prerequisite for predicting and controlling this vibration. Walking loads are the most common type of human-induced loads. Extensive research has been carried out to develop a mathematical model, either deterministic or stochastic, for walking loads based on experimental records of human walking loads. A small

sample includes [3-9] among many others. A comprehensive review of walking load models has been given in [10].

All the above models generally treat ‘a walking pedestrian’ as ‘a moving load’, implying it does not change the dynamic properties of the structure. However, researchers found that human beings do change the dynamic properties including the damping and natural frequency of the structure they occupy [11–14]. This phenomenon is explained by the fact that human beings have their own mass, damping and stiffness, which increases the number of degrees of freedom applicable to the structure through the coupled human-structure interaction (HSI). Clearly, any changes to the properties of the human-structure system are highly related to the properties of the human beings occupying the structure. To investigate this influence, the SMD model and bipedal model are utilized by researchers to model human beings as a mechanical system. Although the bipedal model is able to mirror or duplicate the leg-switching behavior in human walking, and thus can better reflect the strong interaction between the structure and pedestrian [15], it is more complicated and cannot be easily implemented for practical use, while an SMD model can be used for both static and walking people, which gives it the advantage of simplicity.

From the HSI point of view, it is essential to know the model parameters, i.e., natural frequency (or stiffness) and damping ratio, when using the SMD model. Many researchers focused on human SMD parameters for sitting [16-18] and standing [19-21], giving results ranging from 5 Hz to 10.43 Hz and 0.2-0.5, for natural frequency and damping ratio, respectively.

For SMD parameters of walking pedestrian, Shahabpoor [22] adopted the SMD model for walking people from tests of the frequency response function (FRF) on a structure with and without occupants. The natural frequency was given to be 2.75–3 Hz and damping ratio is 0.275–0.3. Nimmen [23] performed tests on a footbridge with people standing on the bridge but in a posture pretending to be walking. The natural frequency of 3.34 Hz and a damping ratio of 0.26 were found. Zhang [24] included the biomechanical forces within the legs to provide input force for the human-structure coupling system, and laboratory experiments were undertaken using force plates and a 3D motion capture system. Natural frequency and biomechanical load factors (BLFs) were found to be related with the walking frequency based on the assumption of a constant damping ratio of 0.3. Note that most SMD model parameters mentioned above are for people in a static status [16-21]. For limited research on effect of walking people on buildings [22-24], some parameters or conditions, i.e., constant damping ratio or walking-like gesture, need to be assumed, which may not be realistic. Moreover, the biomechanical forces are often ignored when identifying the SMD parameters. Therefore, this paper introduces a new method to obtain SMD parameters, together with coefficients for biomechanical forces.

Estimating human model parameters is an output-only inverse dynamic problem, since the inputs are unknown. In recent years, many methods have been proposed to identify input and structural parameters simultaneously from structural responses [25–27]. One popular method is the Kalman filter (KF) method [28], which includes the extended Kalman filter (EKF) and the

unscented Kalman filter (UKF). A development of KF method is the particle filter method [29], where the Gaussian assumption in the traditional Kalman filter is relaxed so that more accurate results can be obtained [30–31]. In this paper, the particle filter method is adopted to identify human model parameters and the unknown biomechanical force input from the ground reaction force obtained experimentally.

2. Spring-mass-damper Model of walking Pedestrian

The SMD model is the simplest model for a pedestrian. It concentrates all the pedestrian mass at the body center-of-mass (COM), resulting in a single-degree-of-freedom system including mass, spring and damper, as shown in Fig. 1. A force couple of equal and opposite biomechanical forces generated by the movement of human muscles is assumed to exist inside the human body to provide excitation force for human model [24]. The SMD model equation of motion for pedestrians is written as

$$M_h\ddot{u} + C_h\dot{u} + K_h u = F_{\text{bio}} \tag{1}$$

in which M_h, C_h, K_h is static human whole body mass, damping and stiffness respectively; F_{bio} is the biomechanical force assumed inside the human body which excites the dynamic system, and u is the displacement response of the body's COM. Following the terminology in biomechanics, the contact force imposed on the ground by the pedestrian is called GRF. Note from Fig.1 that GRF is the summation of spring force, damping force, biomechanical force and the person's body weight. Therefore, once the GRF is measured from an experiment, the response of the SMD

system is the movement of the pedestrian COM, which is

$$\ddot{u} = \frac{\mathrm{GRF} - M_h g}{M_h} \tag{2}$$

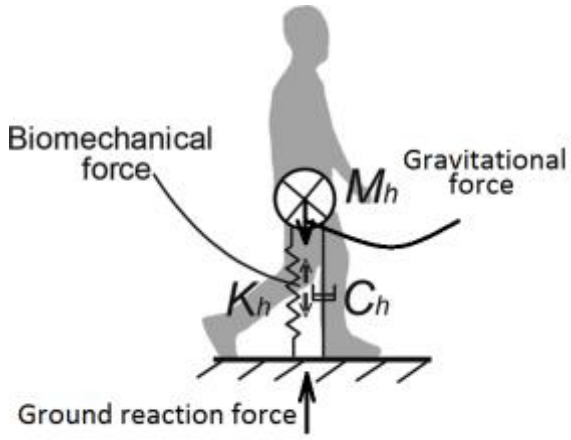

Fig. 1. SMD model of a pedestrian with a pair of biomechanical forces

Observation of normal walking people indicates that gait is a periodic/near-periodic movement of each foot from one position of support to the next position of support in the direction of progression, and the COM moves in a similar periodic pattern. In this connection, it is reasonable to assume the biomechanical force in Eq.1 is periodic and can be expressed in a Fourier series as follows

$$F_{\mathrm{bio}} = a_0 + \sum_{i=1}^{n}\left(a_i \cos(2\pi f_p t) + b_i \sin(2\pi f_p t)\right) \tag{3}$$

where a_0, a_i, b_i are Fourier series coefficients, f_p is the pacing frequency of the pedestrian, and n is the order of the Fourier series model of the biomechanical force, which acts as the input of the human system. The BLF is defined as the ratio between the amplitude of Fourier series and the human weight, which can be expressed as

$$\mathrm{BLF}_i = \sqrt{a_i^2 + b_i^2} \Big/ M_h g \tag{4}$$

3. Theory of Identification

3.1 General Solution

In this study, the human parameters in the SMD model, which is assumed to represent the human body system, are to be identified together with BLFs simultaneously from the measured GRF. This section aims to prove the feasibility of estimating these values at the same time. From Eq. (1) and Eq. (3), the equation of motion of the human system under biomechanical forces is rewritten at each time instant in matrix form as

$$\mathbf{H\Theta} = \mathbf{F} \tag{5}$$

where

$$\mathbf{H} = \begin{pmatrix} \dot{u}(t_1) & u(t_1) & 1 & \sin(2\pi f_p t_1) & \cos(2\pi f_p t_1) & \cdots & \sin(2\pi n f_p t_1) & \cos(2\pi n f_p t_1) \\ \dot{u}(t_2) & u(t_2) & 1 & \sin(2\pi f_p t_2) & \cos(2\pi f_p t_2) & \cdots & \sin(2\pi n f_p t_2) & \cos(2\pi n f_p t_2) \\ \vdots & & & & & & & \\ \dot{u}(t_p) & u(t_p) & 1 & \sin(2\pi f_p t_p) & \cos(2\pi f_p t_p) & \cdots & \sin(2\pi n f_p t_p) & \cos(2\pi n f_p t_p) \end{pmatrix} \tag{6}$$

$$\mathbf{\Theta} = \begin{pmatrix} C_h & K_h & a_0 & a_1 & a_2 & \cdots & a_n & b_n \end{pmatrix}^{\mathrm{T}} \tag{7}$$

$$\mathbf{F} = \begin{pmatrix} -M_h \ddot{u}(t_1) & -M_h \ddot{u}(t_2) & \cdots & -M_h \ddot{u}(t_p) \end{pmatrix}^{\mathrm{T}}. \tag{8}$$

Vector $\mathbf{\Theta}$ includes the parameters to be identified. M_h is assumed as the known value of total human mass, and is thus not included in the vector to avoid multiple-solution problem in the inverse identification. It is also assumed that the human parameters C_h and K_h are constant during walking. The least-square solution of the equations exists and can be expressed as

$$\boldsymbol{\Theta} = (\mathbf{H}^{\mathrm{T}}\mathbf{H})^{-1}\mathbf{H}^{\mathrm{T}}\mathbf{F} \tag{9}$$

3.2 Particle Filter

In the previous section, the procedure for simultaneously estimating human parameters and BLFs was expressed. However, when directly calculating the solution through Eq. 9, it is usually difficult to calculate numerically the inverse of the matrix $\mathbf{H}^{\mathrm{T}}\mathbf{H}$, especially when the matrix is ill-conditioned, which is, unfortunately, always the case. Therefore, a method known as the particle filter is adopted in this paper to identify human parameters and BLFs. This method is briefly reviewed herein.

In the particle filter method, the state of the system is estimated by introducing measured data step by step to the dynamic equation [29–31]. A state-space form of the system dynamic equation is needed for estimating the state, as expressed in

$$\mathbf{x}_{k+1} = f_k(\mathbf{x}_k) + w(k) \tag{10}$$

where $\mathbf{x}_k$ is the state vector representing the state of the system at each time step k. f_k represents the state transition function of the system, and $w(k)$ is the system error with a known distribution. The observation vector $\mathbf{y}_k$ is formed by measurements made at each time step and is related to the state vector through the following observation equation

$$\mathbf{y}_k = h_k(\mathbf{x}_k) + v(k) \tag{11}$$

where $v(k)$ is the observation error with known distribution and independent with the system error $w(k)$. h_k is the transition function from system state vector to observation vector. The expression

of $\mathbf{x}_k$, $\mathbf{y}_k$, f_k and h_k for the human SMD parameter identification problem discussed in this paper are defined in next section.

The main process of particle filter method is to construct the posterior probability density function (PDF) of the state vector through Bayesian state estimation. Two steps known as predict and update are shown in Eq. 12 and Eq. 13, respectively.

$$p(\mathbf{x}_k \mid \mathbf{y}_{1:k-1}) = \int p(\mathbf{x}_k \mid \mathbf{x}_{k-1}) p(\mathbf{x}_{k-1} \mid \mathbf{y}_{1:k-1}) \mathrm{d}\mathbf{x}_{k-1} \tag{12}$$

$$p(\mathbf{x}_k \mid \mathbf{y}_{1:k}) = \frac{p(\mathbf{y}_k \mid \mathbf{x}_k) p(\mathbf{x}_k \mid \mathbf{y}_{1:k-1})}{p(\mathbf{y}_k \mid \mathbf{y}_{1:k-1})} \tag{13}$$

Eq. 12 and Eq. 13 show the procedure to obtain the posterior PDF of time step k. The posterior PDF of time step k-1, $p(\mathbf{x}_{k-1}|\mathbf{y}_{1:k-1})$, with the measurement data up to time step k-1, is passed through the system equation to obtain the prior PDF of time step k expressed as $p(\mathbf{x}_k|\mathbf{y}_{1:k-1})$. Measurement data at time step k is then introduced to calculate the posterior PDF of time step k, $p(\mathbf{x}_k|\mathbf{y}_{1:k})$, based on the Bayesian formula.

Equations 12 and 13 describe the iteration steps in this method. After a number of iteration steps, the system state will converge to the real value. If the transition function f_k and h_k are linear, and the Gaussian distribution assumption applies to both the prior and posterior PDF, only the mean value and covariance of the state need to be estimated at each step. This method is known as the Kalman filter. However, when the parameter identification problem is considered, the transition function f_k is always nonlinear against unknown parameters. Therefore, the assumption of the Kalman filter cannot be applied here. Alternatives to the Kalman filter include the extended Kalman filter (EKF),

the unscented Kalman filter (UKF) and the particle filter (PF), each of which has its own assumptions. In this study, the particle filter method is adopted, since it needs the least assumptions, although it is computationally expensive.

In the particle filter method, the prior and posterior PDF of the state is represented by a large number of particles. When the number of particles becomes large enough, they can equivalently represent the exact PDF in a Monte Carlo way. The Gaussian assumption in EKF and UKF becomes unnecessary because the particles can represent any form of PDF. At each time step k, each particle is passed through the system equation to form a prior PDF. The likelihood of each particle is normalized through Eq. 14, in a process called resampling, where q_i is the normalized likelihood for the i^{th} particle, and N is the number of particles. A new series of particles is generated based on the normalized likelihood and the iteration process continues to the next step until the system state converges to its real value.

$$q_i = p(\mathbf{y}_k \mid \mathbf{x}_k(i)) \Big/ \sum_{i=1}^{N} p(\mathbf{y}_k \mid \mathbf{x}_k(i)) \tag{14}$$

This particle filtering technique is used for identifying human SMD model parameters and BLFs. Instructions for applying this method are given in Section 3.3.

3.3 Application of Particle Filter on SMD Model Identification

When simultaneous identification of human SMD model parameters and BLFs occur, the state vector should include system response terms and unknown parameters. The state vector is shown as.

$$\mathbf{X} = (u, \dot{u}, C_h, K_h, a_0, a_1, b_1, a_2, b_2, \cdots, a_n, b_n)^{\mathrm{T}} \tag{15}$$

$$\dot{\mathbf{X}} = (\dot{u}, \ddot{u}, 0, \cdots 0)^{\mathrm{T}} \tag{16}$$

The equation of motion shown in Eq. 1 should be written in state-space form, as follows.

$$\dot{\mathbf{X}} = \mathbf{A}\mathbf{X} + w \tag{17}$$

in which,

$$\mathbf{A} = \begin{pmatrix} 0 & 1 & 0 & 0 & 0 & 0 & 0 & \cdots & 0 & 0 \\ -\frac{K_h}{M_h} & -\frac{C_h}{M_h} & 0 & 0 & \frac{1}{M_h} & \frac{\cos(2\pi f_p t)}{M_h} & \frac{\sin(2\pi f_p t)}{M_h} & \cdots & \frac{\cos(2\pi n f_p t)}{M_h} & \frac{\sin(2\pi n f_p t)}{M_h} \\ 0 & & & & & \cdots & & & & 0 \\ \vdots & & & & & & & & & \vdots \\ 0 & & & & & \cdots & & & & 0 \end{pmatrix} \tag{18}$$

In matrix **A**, the unknown parameters C_h and K_h are included, so the state equation shown in Eq. 17 is nonlinear, although the linear pedestrian SMD model is adopted. Using the Euler discretization method, Eq. 17 is discretized for numerical computation. The discretized state-space equation of motion is written as.

$$\mathbf{X}_{k+1} = \mathbf{A}_d \mathbf{X}_k + w(k) \tag{19}$$

and

$$\mathbf{A}_d = \mathbf{I} + \mathbf{A}\mathrm{d}t \tag{20}$$

where **I** is the unit matrix.

The observation vector $\mathbf{y}_k$ includes displacement, velocity, and acceleration response of the

pedestrian system

$$\mathbf{y}_k = \left(u_k, \dot{u}_k, \ddot{u}_k\right)^{\mathrm{T}} \tag{21}$$

and is related to the state vector at each time step by

$$\mathbf{y}_k = \mathbf{C}_d \mathbf{X}_k + v(k) \tag{22}$$

where

$$\mathbf{C}_d = \begin{pmatrix} 1 & 0 & 0 & 0 & 0 & & \cdots & & 0 \\ 0 & 1 & 0 & 0 & 0 & & \cdots & & 0 \\ -\frac{K_h}{M_h} & -\frac{C_h}{M_h} & 0 & 0 & \frac{1}{M_h} & \frac{\cos(2\pi f_p t_k)}{M_h} & \frac{\sin(2\pi f_p t_k)}{M_h} & \cdots & \frac{\cos(2\pi n f_p t_k)}{M_h} & \frac{\sin(2\pi n f_p t_k)}{M_h} \end{pmatrix} \tag{23}$$

The particle filter method is applied to the identification problem based on Eqs. 15–23, following the procedure explained in Section 3.2.

4. Numerical Example

To test the feasibility of the proposed method before applying to experimental data, a numerical simulation is conducted. The human body is represented by a SMD model, with mass set to as 75 kg, natural frequency 2.5 Hz and damping ratio 0.4. The damping coefficient c and stiffness k are 942 N·s/m and 18506 N/m, respectively. The input P, i.e., the biomechanical force, is assumed to follow Eq. 24 where

$$P = 300\sin(3\pi t) + 400\sin(4\pi t) + 200\sin(7\pi t) + 100\sin(8\pi t) \tag{24}$$

This input is then expressed using Eq. 3, where n is chosen to be 10. It should be noted here that

1 although a Fourier model with $n = 4$ is usually considered to be enough for modelling human single
2 footfall steps [32], n is set to be 10 to increase modelling accuracy for the purpose of identification.
3 The state vector is generated following Eq. 15. The displacement, velocity and acceleration
4 response of the simulated single-degree-of-freedom system is calculated to form the observation
5 vector at each time step. The method proposed in Section 3 was applied to identify SMD model
6 parameters and the Fourier series simultaneously. With the time interval Δt set to be 0.001 s,
7 Figures 2 and 3 show the converging process of the damping coefficient c and stiffness k at each
8 time step. Figure 4 shows the system input calculated from the identified Fourier series at each time
9 step. As the time steps increase, the parameters and the input converge to the correct value with a
10 small error, which is mainly because the selected input load model is only an approximation of the
11 real input with some modelling error.

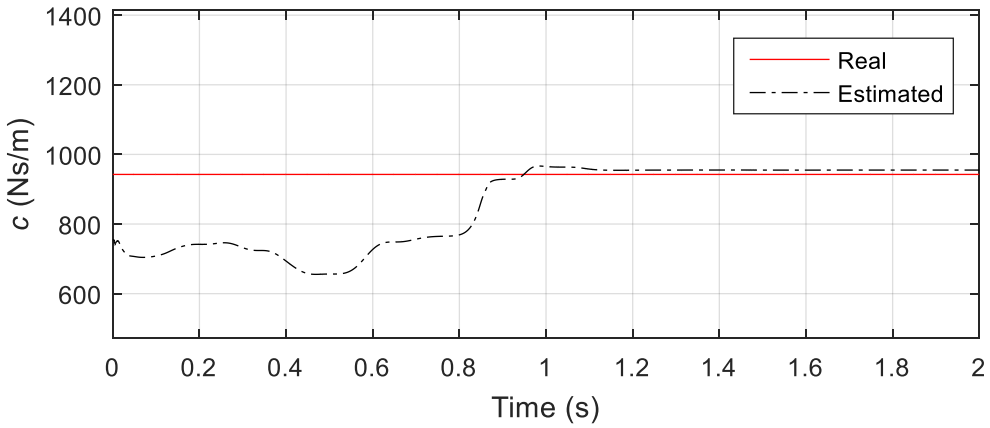

12

13 Fig. 2. Converging process of damping coefficient c

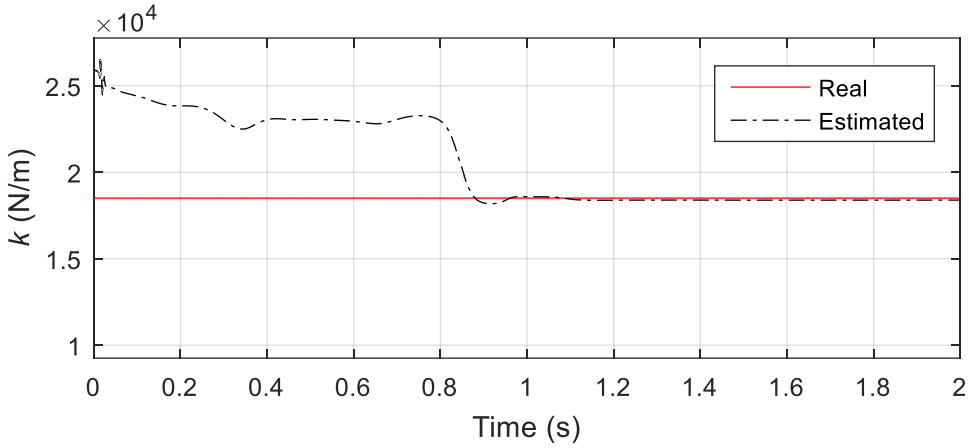

Fig. 3. Converging process of stiffness k

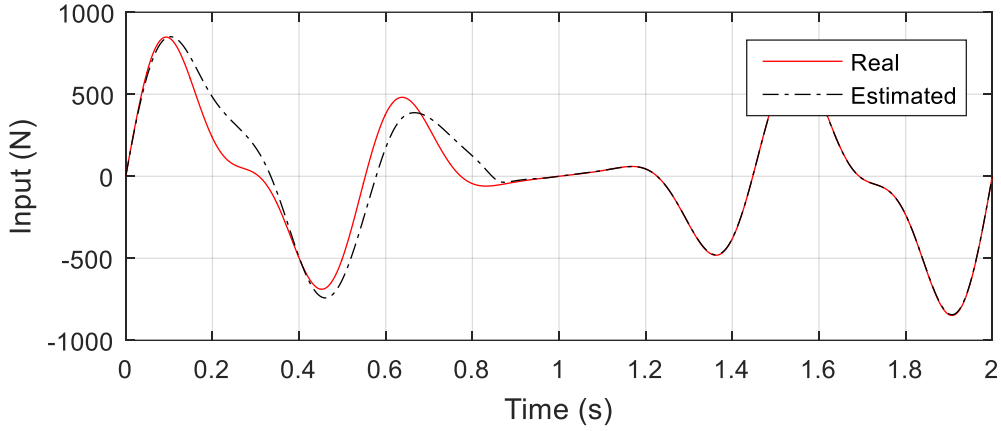

Fig. 4. Converging process of system input F

5. Identification of SMD Parameters experimental using Measured GRFs

5.1 Experimental identification of pedestrian GRF

An experiment was conducted to estimate the parameters of the SMD model and the biomechanical force using the method stated above. The test participant was equipped with an insole sensor system (Novel Pedar System, Germany), which was used to measure the continuous GRF of the participant and to transmit signals to a nearby data acquisition PC wirelessly through the Bluetooth technique. The validity and accuracy of this insole sensor system are well acknowledged [33-35].

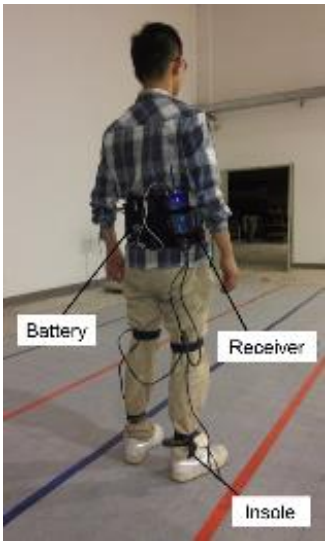

Fig. 5. Experiments of GRF using the insole pressure measurement system

Participants were asked to walk along a 40m×1.5m rigid track prompted by a metronome. In a total of 11 cases, pacing frequencies adopted were eight fixed frequencies, i.e., 1.5, 1.65, 1.75, 1.8, 1.95, 2, 2.1 and 2.25 Hz, and three pacing frequencies chosen by participants at their own preferences of slow, normal and fast. Each pacing frequency case was repeated two or three times to ensure repeatability. Fifty-six people participated in this experiment and 1528 records of ground reaction forces were obtained. Selection of participants and the test protocol satisfied the requirements given by Tongji Metical Ethics Committee. Table 1 summarizes participant information.

Table. 1. Ages, weight and height information for participants

Sex	Number	Age (yrs)			Weight(kg)			Height(cm)		
		Mean	SD	Range	Mean	SD	Range	Mean	SD	Range
Male	39	24.0	2.52	19.8-28.9	68.3	15.00	49.8-95.1	174.6	47.58	156-197
Female	17	23.7	6.37		60.3	4.98		162.6	21.28	

Note: SD refers to standard deviation

One typical GRF record of 1.75 Hz pacing frequency is shown in Fig. 6. The force recorded by

left and right sensors are added together to form the total GRF and then used to calculate COM response. The time history of GRF has the feature of near-periodic while differences in each step can be observed, which resembles those measured by other researchers [32].

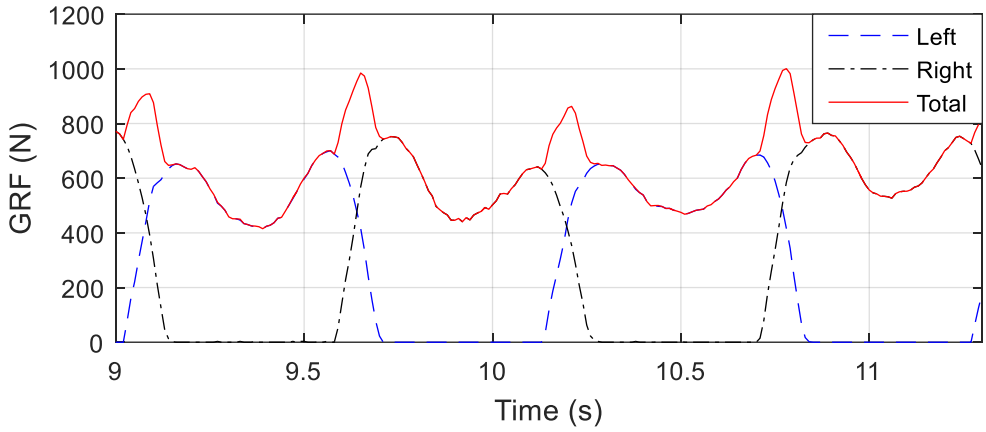

Fig. 6. Typical experimental record (pacing frequency = 1.75 Hz)

5.2 Data processing and parameter identification procedure

The acceleration response of the COM was calculated from GRF records through Eq. 2 and filtered with a high-pass cut-off frequency of 0.15 Hz. Displacement and velocity responses were obtained through integration by trapezoidal rule, and were then used to form the observation vector for Eq. 21. Because the Fourier coefficients of biomechanical force could be different between each step, the calculated COM acceleration time histories were divided into pieces of single footfall steps, i.e., peak to peak in the time history curve. The velocity and displacement responses were also divided accordingly. A similar technique was once used by Ding et al. [36] to identify earthquake input assuming that the earthquake parameters in a short duration remained constant. For parameter identification using each piece of single footfall steps, particles representing the initial state

distribution of human damping, stiffness and response terms, remained the same as those recorded in the last step of the previous piece, while the particles for the Fourier series terms were regenerated at the beginning of each piece.

Following the above process, the particles were passed through prediction and update Eqs. 19 and 22. For the SMD parameter C_h and K_h, the standard deviation of system error $w(k)$ was set to be 5 N·s/m and 100 N/m, respectively, which is around 1% of the nominal values. This aims to prevent C_h and K_h from getting frozen (i.e., converging to a wrong value before reaching the correct value) in the particle filtering process. For the response terms in the state vector, the standard deviation of $w(k)$ was empirically set at 0.5% of the RMS value of each state quantity to compensate for the incompleteness coming from the dynamic model and the discretization during calculation [37]. Although the influence of $w(k)$ on the estimation process was not theoretically investigated, the robustness of estimation results was found against slight changes of $w(k)$ values. The observation error term $v(k)$ for measured acceleration, velocity and displacement was taken as 10% of the RMS values of the respective state quantities to account for the influence of sensor noise.

5.3 Identification Results of an Individual

Fig. 7 and 8 show the identification convergence curve of damping and stiffness for a participant walking at 1.75 Hz. The range of initial uniform distribution is set from 400-1000 N·s/m and 12000-20000 N/m for damping coefficient and stiffness, respectively. It should be noted that the estimated values are not limited within this range. It is found that the estimation result is robust

against the initial range of distribution. At each time step, the estimated value is calculated as the mean value of all particles. The damping coefficient and stiffness converge to a fixed value after around two seconds, which is 200 iteration steps of 0.01 s time interval. The converged value for damping and stiffness are 434 N·s/m and 8940 N/m, respectively. With the human participant mass of 58 kg, these values give the human damping ratio value as 0.29 and natural frequency as 1.94 Hz.

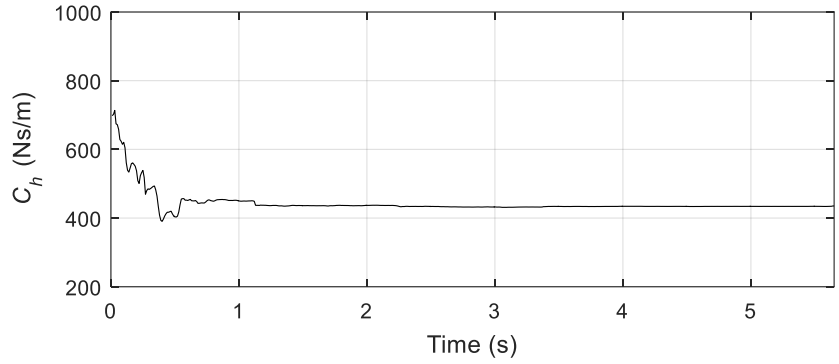

Fig. 7. Estimating result for damping coefficient C_h

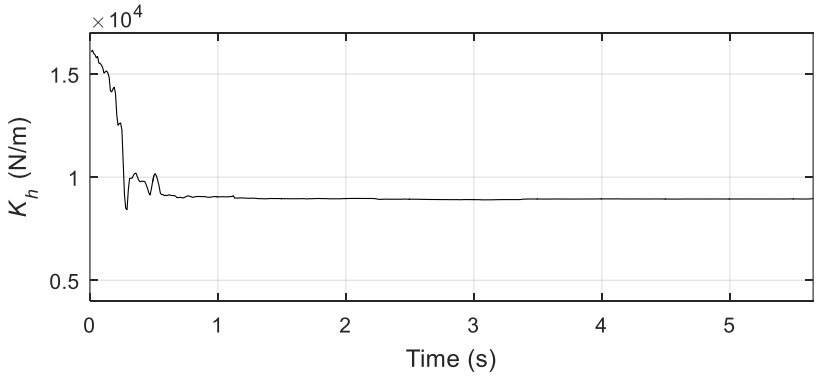

Fig. 8. Estimating result for stiffness K_h

Having damping and stiffness identified with known body mass and COM response including COM displacement, velocity and acceleration, the biomechanical force time history can be directly calculated from Eq. 1. The result is shown in Fig. 9 where it is observed that the biomechanical

force is a near-periodic process. In frequency domain (Fig. 10) the Fourier amplitudes indicate the BLF with values of the first three orders $BLF_1 = 0.212$, $BLF_2 = 0.042$, and $BLF_3 = 0.049$.

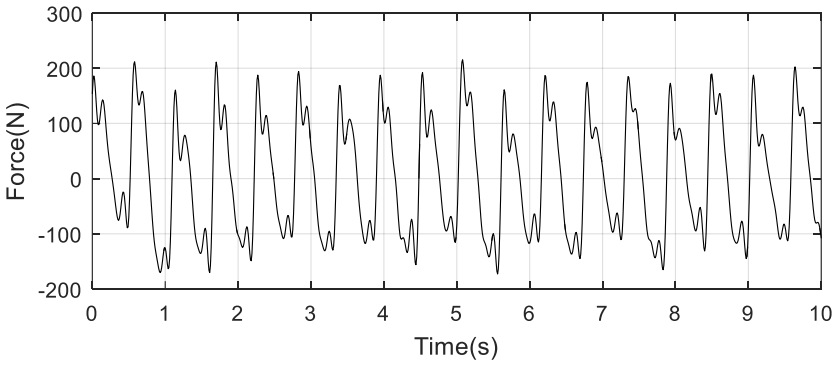

Fig. 9. Time history of biomechanical forces

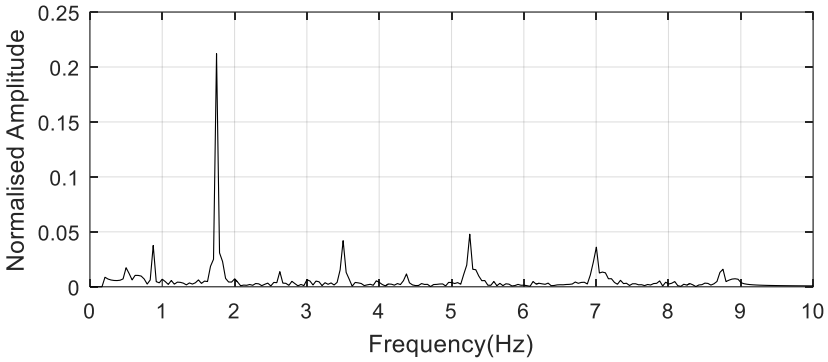

Fig. 10. Fourier amplitudes of biomechanical forces

Figures 11a and 11b show the variation of natural frequency and damping ratio with pacing frequency, respectively, for all test cases of the same participant. An increasing trend for natural frequency and a decreasing trend for damping ratio can be observed.

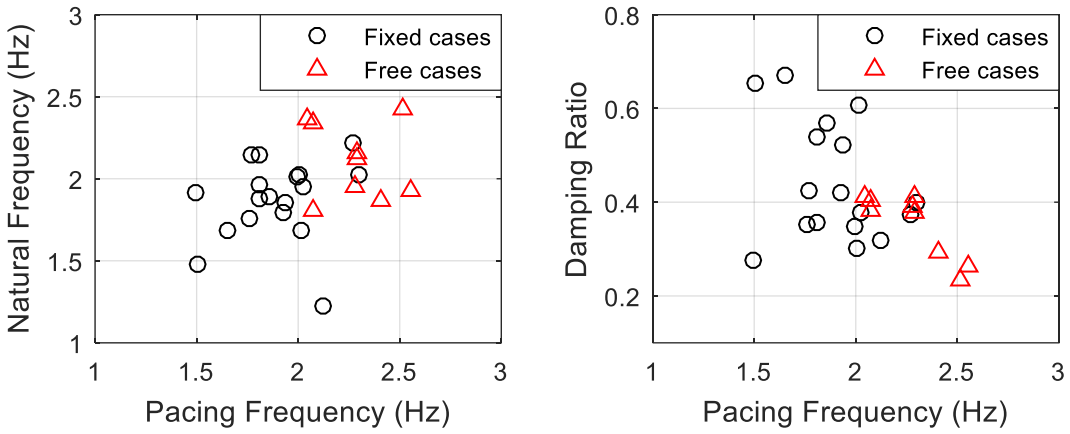

(a) Natural Frequency (b) Damping ratio

Fig. 11 Variation of SMD parameters with pacing frequency (one pedestrian)

5.4 Statistical Analysis

All 1528 records of the continuous walking load were processed by the above proposed method to identify the SMD parameters. The results of natural frequency, damping ratio and BLF_1 are shown in Figures 12(a)–(c) against the pacing frequency. A linear relation was fitted for mean values of natural frequency, damping ratio, and BLF_1. As the pacing frequency becomes larger, natural frequency and first-order BLF increases accordingly, while the damping ratio tends to decrease. The fitting equation is also given in Fig. 12.

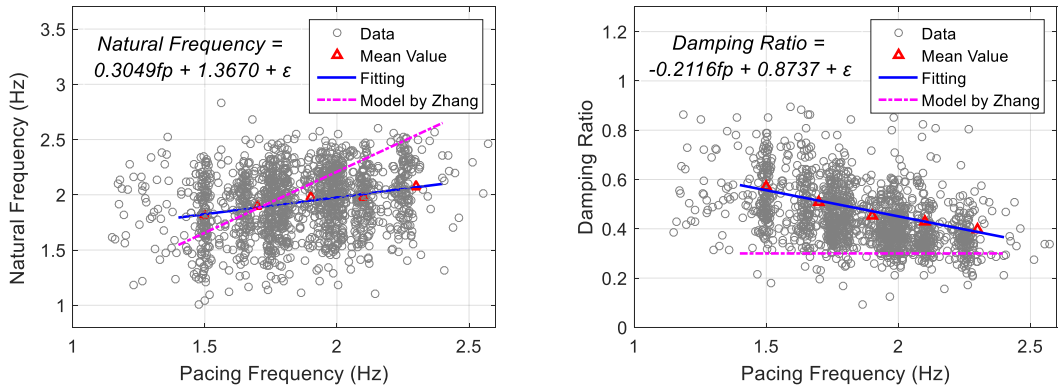

(a) Natural frequency (b) Damping ratio

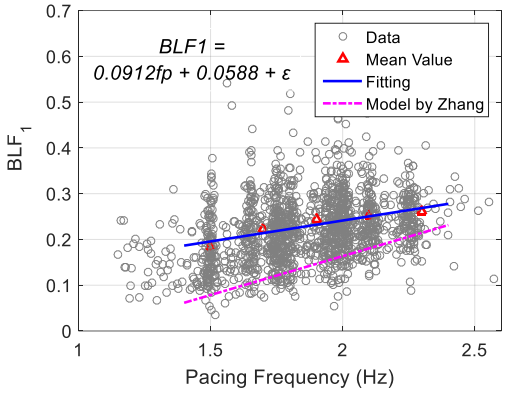

(c) First-order BLF

Fig. 12. Linear fitting for mean values of SMD parameters with pacing frequency

The model error terms ε, for natural frequency, damping ratio and BLF_1, were all found following a normal distribution with the mean value and standard deviation value summarized in Fig. 13(a)–(c), together with the PDF from the experiment data.

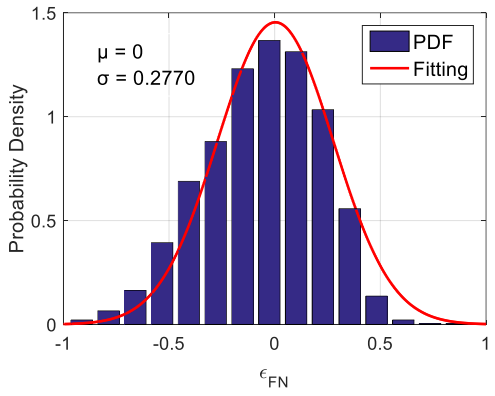

(a) Natural frequency

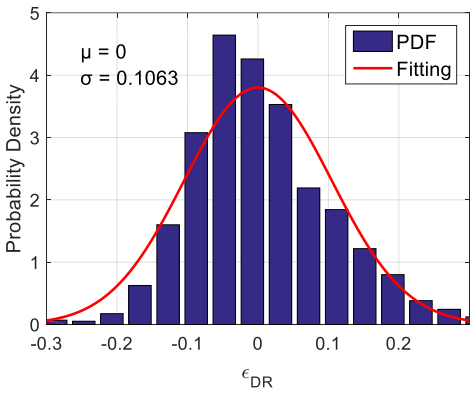

(b) Damping ratio

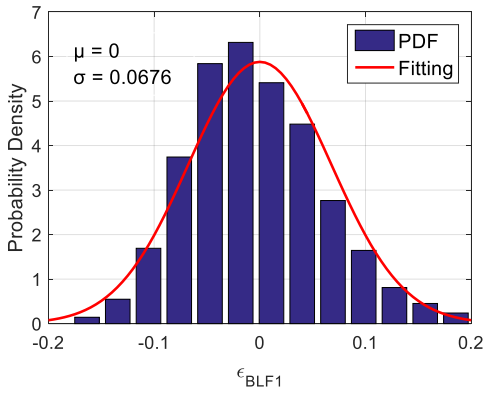

(c) First-order BLF

Fig. 13. Normal distribution fitting for model error terms

For higher order coefficients of biomechanical force, i.e. BLF_2 and BLF_3, no clear relation was found with pacing frequency. A logarithmic normal distribution was fitted to the second and third order of BLFs, as shown in Fig. 14(a)–(b).

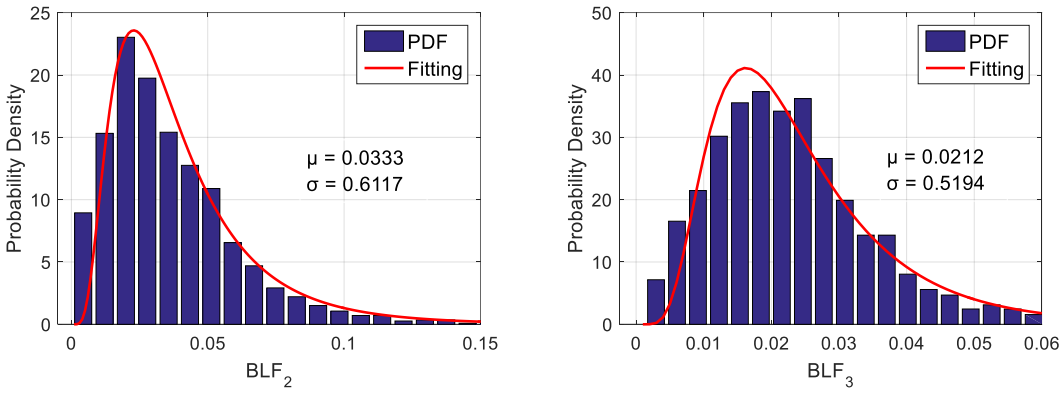

(a) Second-order BLF (b) Third-order BLF

Fig. 14. Logarithmic normal distribution fitting for second and third order BLF

5.5 Comparison With Results from Other Researches

The estimated SMD parameters of this study are summarized and compared with results from other researchers in Table 2. For most of them, human natural frequency and damping ratio remains constant. Only one model [24] proposed the model parameter to be linearly related with pacing frequency, as found in this paper. The linear trend in [24] is compared in Fig. 12(a)–(b). The mean values of natural frequency for pacing frequency 1.5-2.5 Hz are 1.82-2.13 Hz, which are smaller than those reported for sitting and standing person. The identified damping ratios are 0.56-0.34 for pacing frequency 1.5-2.5Hz, which are in the variation range of reported data.

Table. 2. Comparison with results from other researchers

Source	Posture	Natural Frequency (Hz)	Damping Ratio
Wei 1998 [16]	Sitting	5.0	0.45
Falati 1999 [17]	Sitting	10.43	0.45-0.55
Sachse 2002 [18]	Sitting	5.5–8.3	0.33–0.35
Brownjohn 1999 [19]	Standing	5.1	0.38
Zheng 2001 [20]	Standing	5.24	0.39
Matusmoto 2003 [21]	Standing	5.74	0.695
Shahabpoor 2016 [22]	Walking	2.75–3	0.275–0.30
Van Nimmen 2015 [23]	Walking	3.34	0.26
Zhang 2015 [24]	Walking	$1.1043\,f_p$	0.30
This Study	Walking	$0.3049f_p + 1.3670$ (1.82–2.13 for $f_p = 1.5$–2.5)	$-0.2116f_p + 0.8737$ (0.56–0.34 for $f_p = 1.5$–2.5)

Note: f_p refers to pacing frequency

The results of BLFs for walking pedestrians, to the best of the authors' knowledge, are rarely reported. The only result found in literature is proposed in [24], in which the first-order of BLF has a linear relationship against pacing frequency, while the second and third BLF were fitted by a generalized extreme value distribution in accordance with the results found in this paper. The linear trend for first-order BLF from [24] is compared with the present result in Fig. 12(c).

6. Conclusions

When structures are excited by pedestrians, the HSI phenomenon occurs. Through this interaction, the human-structure system dynamic properties are changed by pedestrians occupying the structure. Although researchers have found that the change to structural parameters is related to human biomechanical properties, the human parameters have not been fully studied. In this paper, the pedestrian is modeled using a SMD model with a pair of biomechanical forces, where the

natural frequency and damping ratio of this model are investigated. Wireless force insoles were applied and equipped to test participants to obtain a continuous GRF induced by human walking. Based on the measured data, the parameters of an SMD model and a biomechanical force are simultaneously identified using a time-domain approach known as the particle filter method. Natural frequency, damping ratio and first-order BLF of the SMD model were found to have a close relation with walking frequency and a linear model was fit. For a higher order of BLF, a logarithmic normal distribution was used to fit the experimental data.

The results obtained in this paper are compared with those from other researches. Close relationship is found between results using different methods, showing the validity of the findings in this paper. The results can serve as the basis for further investigation on parameter identification for pedestrians on an oscillating structure, where the human-structure interaction may occur. It is also proved that the system identification method is capable of dealing with human parameter identification problem, which is not much addressed before. Moreover, the experimental data of human walking load time histories can serve as the database for further research on human-induced load and vibration.

Acknowledgement

The authors would like to acknowledge the financial support provided by National Natural Science Foundation of China (51478346) and State Key Laboratory for Disaster Reduction of Civil Engineering (SLDRCE14-B-16).

REFERENCES

[1] P. Dallard, A.J. Fitzpatrick, A. Flint, S. Le Bourva, A. Low, R.M. Ridsdill Smith, M. Willford, The London Millennium Footbridge, in: Structural Engineer, 2001: pp. 17–33.

[2] J.M.W. Brownjohn, S. Zivanovic, A. Pavic, Crowd dynamic loading on footbridges, Footbridge 2008.

[3] F.W. Galbraith, M. V. Barton, Ground Loading from Footsteps, The Journal of the Acoustical Society of America. 48 (1970) 1288.

[4] S.V. Ohlsoon, C. T. H. Gskola, Floor vibrations and human discomfort, Chalmers University of Technology, Division of Steel and Timber Structures, 1982

[5] A. Ebrahimpour, A. Haman, R.L. Sack, W.N. Patten, Measuring and modeling dynamic loads imposed by moving crowds, Journal of Structural Engineering. 122 (1996) 1468–1474.

[6] S.C. Kerr, N.W.M. Bishop, Human induced loading on flexible staircases, Engineering Structures. 23 (2001) 37–45.

[7] J.M.. Brownjohn, A. Pavic, P. Omenzetter, A spectral density approach for modelling continuous vertical forces on pedestrian structures due to walking, Canadian Journal of Civil Engineering. 31 (2004) 65–77.

[8] S. Živanović, A. Pavić, P. Reynolds, Probability-based prediction of multi-mode vibration response to walking excitation, Engineering Structures. 29 (2007) 942–954.

[9] Y. Peng, J. Chen, G. Ding, Walking load model for single footfall trace in three dimensions

based on gait experiment, Structural Engineering and Mechanics. 54(5), 937-953.

[10] V. Racic, A. Pavic, J.M.W. Brownjohn, Experimental identification and analytical modelling of human walking forces: Literature review, Journal of Sound and Vibration. 326 (2009) 1–49.

[11] T. Ji, B.R. Ellis, Human-Structure Interaction in Vertical Vibrations., Proceedings of the ICE - Structures and Buildings. 122 (1997) 1–9.

[12] A. Cappellini, S. Manzoni, M. Vanali, Quantification of damping effect of humans on lightly damped staircases, in: Topics in Dynamics of Civil Structures - Proceedings of the 31st IMAC, A Conference on Structural Dynamics, 2013, 2013: pp. 453–460.

[13] M.J. Griffin, J. Erdreich, Handbook of Human Vibration, The Journal of the Acoustical Society of America. 90 (1991) 2213.

[14] K.A. Salyards, N.C. Noss, Experimental Evaluation of the Influence of Human-Structure Interaction for Vibration Serviceability, Journal of Performance of Constructed Facilities. 28 (2014) 458–465.

[15] M. Bocian, J.H.G. Macdonald, J.F. Burn, Biomechanically inspired modeling of pedestrian-induced vertical self-excited forces. Journal of Bridge Engineering, 18.12(2013) 1336-1346.

[16] L. Wei, M.J. Griffin, Mathematical Models for the Apparent Mass of the Seated Human Body Exposed To Vertical Vibration, Journal of Sound and Vibration. 212 (1998) 855–874.

[17] S. Falati, The contribution of non-structural components to the overall dynamic behavior of

concrete floor slabs. University of Oxford New College, 1999.

[18] R. Sachse, The influences of human occupants on the dynamic properties of slender structures. University of Sheffield, 2003.

[19] J.M.W. Brownjohn, Energy dissipation in one-way slabs with human participation. Proceedings of the Asia-Pacific Vibration Conference. Nanyang Technological University, Singapore, December, 2009.

[20] X. Zheng, J.M.W. Brownjohn, Modeling and simulation of human-floor system under vertical vibration. International Society for Optics and Photonics, 2001, 513-520

[21] Y. Matsumoto, M.J. Griffin, Mathematical models for the apparent masses of standing subjects exposed to vertical whole-body vibration, Journal of Sound and Vibration. 260 (2003) 431–451.

[22] E. Shahabpoor, A. Pavic, V. Racic, Identification of mass-spring-damper model of walking humans, Structures. 5 (2016) 233–246.

[23] K. Van Nimmen, K. Maes, S. Živanović, G. Lombaert, G. De Roeck, P. Van den Broeck, Identification and modelling of vertical human-structure interaction, in: Conference Proceedings of the Society for Experimental Mechanics Series, 2015: pp. 319–330.

[24] M. Zhang, C.T. Georgakis, J. Chen, Biomechanically Excited SMD Model of a Walking Pedestrian, Journal of Bridge Engineering. (2016) C4016003.

[25] H. Sun, R. Betti, Simultaneous identification of structural parameters and dynamic input with incomplete output-only measurements, Structural Control and Health Monitoring. (2013) n/a-n/a.

[26] J. Chen, J. Li, Simultaneous identification of structural parameters and input time history from output-only measurements, Computational Mechanics. 33 (2004) 365–374.

[27] M.J. Perry, C.G. Koh, Output-only structural identification in time domain: Numerical and experimental studies, Earthquake Engineering & Structural Dynamics. 37 (2008) 517–533.

[28] R.E. Kalman, A New Approach to Linear Filtering and Prediction Problems, Journal of Basic Engineering. 82 (1960) 35. doi:10.1115/1.3662552.

[29] N.J. Gordon, D.J. Salmond, a. F.M. Smith, Novel approach to nonlinear/non-Gaussian Bayesian state estimation, IEE Proceedings F Radar and Signal Processing. 140 (1993) 107.

[30] M.S. Arulampalam, S. Maskell, N. Gordon, T. Clapp, A tutorial on particle filters for online nonlinear/non-Gaussian Bayesian tracking, IEEE Transactions on Signal Processing. 50 (2002) 174–188.

[31] J. Carpenter, P. Clifford, P. Fearnhead, Improved particle filter for nonlinear problems, IEE Proceedings - Radar, Sonar and Navigation. 146 (1999) 2.

[32] V. Racic, and J.M.W. Brownjohn, Stochastic model of near-periodic vertical loads due to humans walking. Advanced Engineering Informatics 25.2 (2011) 259-275.

[33] H.L.P. Hurkmans, J.B.J. Bussmann, R.W. Selles, H.L.D. Horemans, E. Benda, H.J. Stam, J.A.N. Verhaar. Validity of the Pedar Mobile system for vertical force measurement during a seven-hour period. Journal of Biomechanics 39.1 (2006) 110-118.

[34] S. Barnett, J.L. Cunningham, S. West. A comparison of vertical force and temporal parameters

produced by an in-shoe pressure measuring system and a force platform. Clinical Biomechanics 16.4 (2001) 353-357.

[35] K. Nakazato, P. Scheiber, E. Müller. A comparison of ground reaction forces determined by portable force-plate and pressure-insole systems in alpine skiing. Journal of Sports Science and Medicine 10.4 (2011) 754-762.

[36] Y. Ding, B. Zhao, B. Wu, X. Zhang, L. Guo, Simultaneous identification of structural parameter and external excitation with an improved unscented Kalman filter, Advances in Structural Engineering 18.11(2015) 1981-1998.

[37] K. Matsuoka, K. Kaito, M. Tokunaga, T. Watanabe, M. Sogabe, Estimation of bridge deflection response under passing train loads based on acceleration. Structural Engineering and Earthquake Engineering, 69 (2013) 527-542.

List of Figure Captions

List of Table Captions